Binary Black Hole Formation in the Galactic Center

Renhao Liang (s3663442), Xueyang Hu (s2788322),
Yi Kang (s2881039)

January 3, 2023

Abstract

Most discovered gravitational wave events now are attributed to mergers of black holes. The galactic center would be an ideal place to produce binary black holes (BBHs) as there are abundant stars and also black holes. We simulate the dynamics of black holes (BHs) and gas in the galactic center with `AMUSE`, study the BBH formation in the gas-free and gaseous scenarios. We also study if a gas disk could influence the BBH hardness, the angular momentum directions, or the distance to the SMBH. The influence of the properties of the gas disk on the BBH formation efficiency is also studied in our project.

1 Introduction

The gravitational wave event has been a hot topic in astrophysics since the first gravitational wave signal detected by the Laser Interferometer Gravitational Wave Observatory (LIGO) (Abbott et al., 2016). As waves of the intensity of gravity of accelerated masses, gravitational waves are so weak that so far we can only detect those from the mergers of black holes and neutron stars by large interferometers, e.g., LIGO, VERGO, and KAGRA. And most detected gravitational wave events (38 among the 52 identified) are considered to be black hole mergers according to the mass estimation (Abbott et al., 2019, 2021, The LIGO Scientific Collaboration et al., 2021).

Binary black holes (BBHs) are therefore important sources of gravitational wave events.

Potential channels to produce BBHs attracts our attention. As the relative velocities of the BHs are remarkable, independent BHs have to lose energy to form binaries. In the gas-free environment, BBHs can be formed via gravitational scattering: pairing BHs eject a third object to slow down themselves and then get captured by each other (e.g., Portegies Zwart and McMillan (2000)). While in an extremely condense gaseous environment around a SMBH, BHs would slow down via friction with the gas McKernan et al. (2012, 2014). Other mechanisms have also been proposed, like chemical homogeneous evolution (Mandel and de Mink, 2016, Marchant et al., 2016) and the Lidov-Kozai effect (e.g. Liu et al. (2019)). In this project, we focus on the gravitational effects of the hydrodynamic components. Considering the SMBH, stellar-mass BHs and interstellar medium (ISM), we simulate the BBH formation and study what parameters of the gas in simulations can influence the formation of BBHs.

2 Methods

To study how gas disk influence the formation of BBHs, we simulate the dynamics of stellar-mass BHs in two different scenarios with `AMUSE` (Portegies Zwart and McMillan, 2018, Portegies Zwart et al., 2013, Pelupessy et al., 2013, Portegies Zwart et al., 2009). The first scenario is stellar-mass BHs surrounding a central SMBH with no gas. The system is completely N-body in which only the gravity of other BHs can affect the formation of BBHs, and we use N-body code `ph4` (Portegies Zwart and McMillan, 2018) in the simulation. The second scenario is stellar-mass BHs along with a gas disk surrounding a central SMBH, in the simulation of which we introduce gas particles to the same BHs in the former case with `Fi` code (Hernquist and Katz, 1989, Pelupessy et al., 2004, Pelupessy, 2005, Gerritsen and Icke, 1997), and bridge it with the `ph4` code to bring in the effects of hydrodynamics and consider the interaction between BHs and gaseous environment. Through comparing the results of the simulations of the two scenarios, we can obtain the effect of gas disk on the process of BBH formation in galactic center. We further alter some properties of the gas disk to check how these properties impact the BBH formation.

The BHs are set up as follows: the central supermassive black hole

(SMBH) has mass $4.154 \times 10^6\ M_{\mathrm{SUN}}$, equivalent to the mass of the Sagittarius A* (GRAVITY Collaboration et al., 2019). For the ordinary BHs, 300 masses are sampled from a power law distribution within $[1\ M_{\mathrm{SUN}}, 100\ M_{\mathrm{SUN}}]$ with a power of -2.35 following Salpeter power-law stellar initial mass function (Salpeter, 1955). Then the dynamical model is established by the `ProtoPlanetaryDisk` function of `AMUSE`, which uniformly distributes the 300 BHs within an annulus between $[1\ \mathrm{pc}, 10\ \mathrm{pc}]$ to the SMBH on the X-Y plane and the distribution on the perpendicular Z axis is restricted (within 0.1 pc in thickness). The BHs all have Kepler orbits around the SMBH, with $v_z = 0$. Besides, the radii of BHs are their Schwarzschild radii, $2GM/c^2$. The gas particles are also initialized with `ProtoPlanetaryDisk`, and added to the BHs in the Bridge experiment. As our goal is to study the effect of gas on the formation of BBHs, we set the relevant parameters as variables and fix the initial conditions of the BHs. The number of gas particles is a variable N_{gas}, and the gas particle mass M_{gas} as a fraction of the mass of the SMBH. Each gas particle has the same mass, and the radii are computed by assuming they are spheres with a uniform density of 3 g cm^{-3}. We set $N_{\mathrm{gas}} = 1000$ and $M_{\mathrm{gas}} = 10^{-6}\ M_{\mathrm{SMBH}} = 4.154\ M_{\mathrm{SUN}}$ as the reference. Figure 1 shows the initialization of the system with these parameters, with all BHs and gas particles. A reasonable set of experiments should grid the two parameters. However, due to limited time, we can only marginalize the study, focusing on each parameter respectively. To study the effect of the gas particle mass, we fix N_{gas}, and select $M_{\mathrm{gas}}/M_{\mathrm{SMBH}}$ to 10 to the power of every 0.2 from -7 to -5 ($\{-7.0, -6.8, -6.6, ..., -5.0\}$). To study the effect of the number of gas particles, we fix M_{gas} and change N_{gas} so that the total gas masses are the same as in the previous experiments.

However, more setups are needed to run the simulation. When some BH particles get too close, the time interval decreases infinitely and the simulation is stuck. Therefore, we enable a collision detection and resolve algorithm. Once the distance between two BH particles are within 10^5 times of the sum of their radii, we delete the two BHs and create a new BH particle whose mass is the sum of the two, and its position and velocity are the same as the center of mass of the two. In fact, collision rarely happens in our experiments, and this setup is just to prevent converged evolving time.

The binaries are detected based on the `get_binaries` function in `AMUSE`,

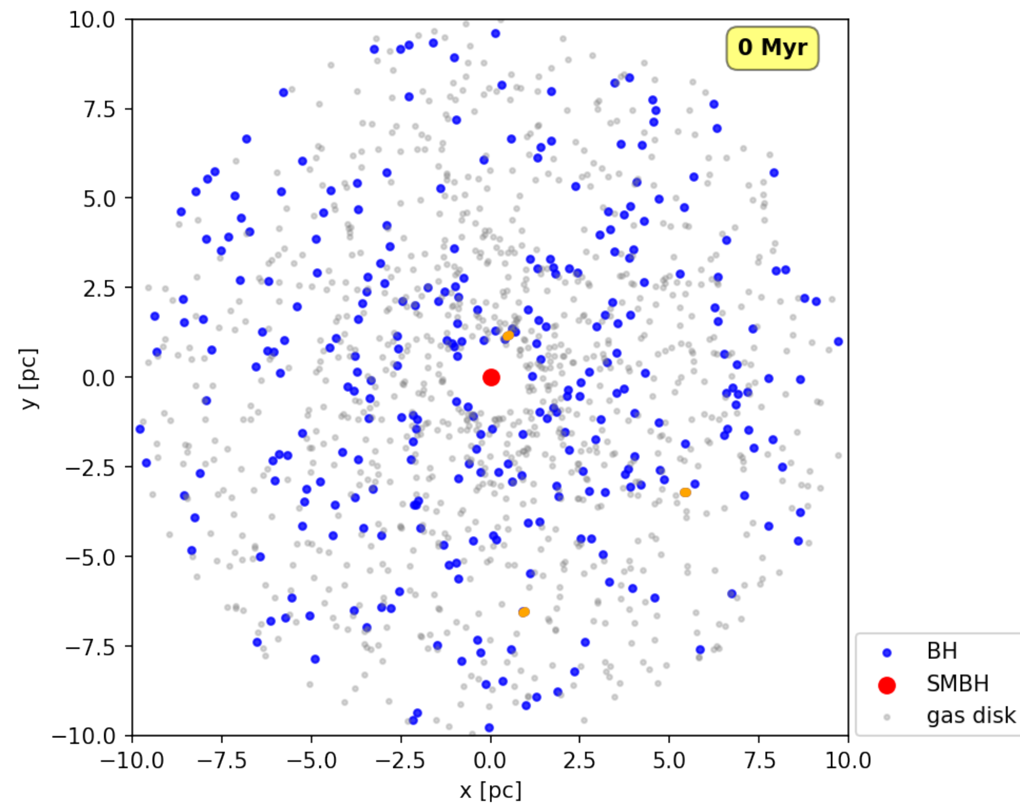

Figure 1: The initial positions of the SMBH (red), BHs (blue) and gas particles (grey) on the X-Y plane. The orange dots are those already identified as soft binaries (0.5<hardness<10).

in which two BH particles are identified as a binary only if

$$\frac{G(M_1 + M_2)}{|\mathbf{r}_1 - \mathbf{r}_2|} - \frac{1}{2}(\mathbf{v}_1 - \mathbf{v}_2)^2 > \text{hardness} \cdot E_m(\frac{1}{2}\mathbf{v}^2), \tag{1}$$

where $E_m(\frac{1}{2}\mathbf{v}^2)$ is the average kinetic energy weighted by mass in the system. This inequation means two BHs need to be massive enough or close enough to be identified as binaries, or the relative velocity should be small. To increase sensitivity we set hardness $= 0.5$. For every binary, we also define a hardness by replacing the greater than sign by an equal sign in eqn. 1. We define $0.5 <$ hardness < 10 as soft binaries, and hardness > 10 as hard binaries.

We first run simulations to 80 Myr for both the N-body scenario and

Bridge scenario. The parameters of the gas disk are the reference values described earlier. We also resolve the BH collisions during the evolving, meanwhile we detect the binaries at every 1 Myr to speed up the simulations. This is a large time step, as the period of the innermost orbits ($r = 1$ pc) is $T \approx 0.05$ Myr. However, as the BHs residing in the inner orbits have significant (relative) velocities and thus difficult to form binaries, we could largely neglect them. And the outermost orbits has a period of $T \approx 1.45$ Myr. Therefore, the time step should be sufficient to capture the dynamics of these BHs. When binaries are detected, we record their mass, relative distance and velocity, hardness, direction of the binary angular momentum and the location of the binary in the disk.

To study the effects of the gas disk in detail, we also run another short-term simulations. In these simulations, we detect binaries with a time step of 1 Myr. We only evolve the model to 5 Myr, as we find most (soft) BBHs are formed at the very beginning in the former long-term simulations, and hardly survive longer than several Myrs. Note that in our detection method, the same binary presented at more than one snapshots are counted for multiple times. It is reasonable that it can reflect the ability of maintaining BBH formation of a system. Simulations of every selection of the $\{M_{\text{gas}}, N_{\text{gas}}\}$ pair are run for 20 times, and we compute the means and standard deviations (std) of the number of binaries and hardness.

3 Simulation Results

Before examining the results, we first check the binary detection sensitivity. In eqn. 1, the sentivity is directly related to the average kinetic energy. The `ProtoPlanetaryDisk` function assumes Kepler orbits, and the SMBH is much more massive than the sum of the other components in the system. Therefore, the BHs are ruled by the gravity of the SMBH, and the system can be regarded stable. The average kinetic energy should not change remarkably unless many collisions happen, which is not the fact in our experiments. As a result, the sensitivity of the binary detection algorithm is constant and stable in our experiments.

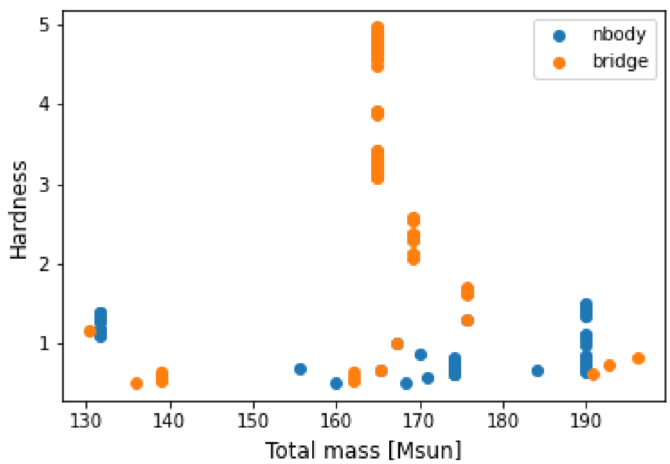

Figure 2: The hardness and total mass of the detected binaries in the 80 Myr runs. The result of the N-body scenario is colored in blue and the Bridge in orange.

3.1 N-body vs Bridge: an Example Run

In this section we present the result of an example 80 Myr run of an N-body simulation and a Bridge simulation with the same BH initial conditions, as all the other runs show similar results.

We found 81 binaries in the N-body experiment and 96 binaries in the Bridge experiment. From Figure 2 we find that all binaries are soft. In fact, hard binaries are rarely seen in our simulations, with an estimated frequency of 2 in 15 runs. But the Bridge scenario indeed exhibits harder binaris than the N-body. This plot also shows that massive BHs are more likely to form BBHs as the total mass of the binaries are all above 120 $M_{\rm SUN}$, compared with the mass distribution of BHs described in the previous section. This is expected from eqn. 1. Moreover, from eqn. 1, it is seen that a small relative distance or small relative velocity can either let two BHs to be identified as a binary. We show the two properties in Figure 3 and find it is the small relative distance that dominants the identification.

Furthermore, we plot the BBH properties, i.e. the angle between the binary angular momentum (AM) and the Z-direction, and their distance to the SMBH in Figure 4. The two distributions show no preference between

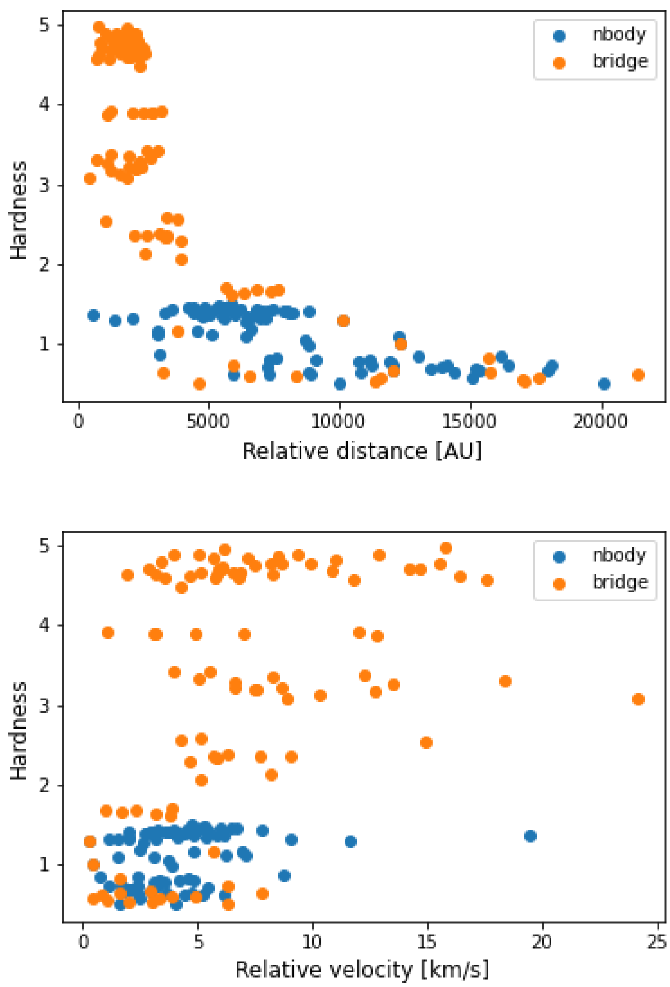

Figure 3: The hardness and relative distance (top) and velocity (bottom) of the detected binaries in the 80 Myr runs. The result of the N-body scenario is colored in blue and the Bridge in orange.

the N-body and Bridge scenarios.

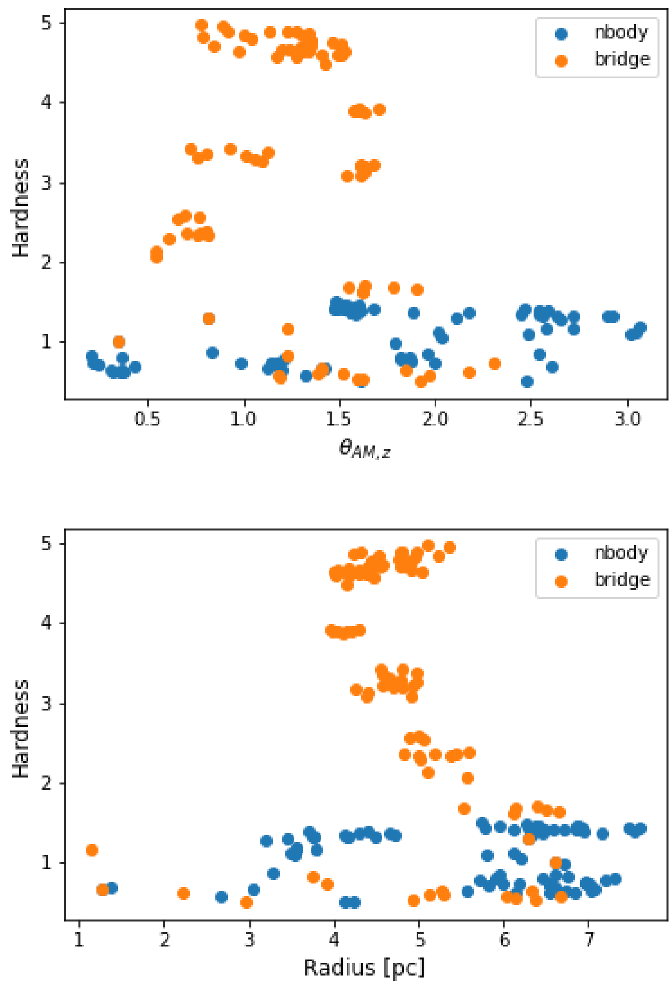

Figure 4: The hardness and angle between the binary AM and the Z-direction (top) and the distance to the SMBH (bottom) of the detected binaries in the 80 Myr runs. The result of the N-body scenario is colored in blue and the Bridge in orange.

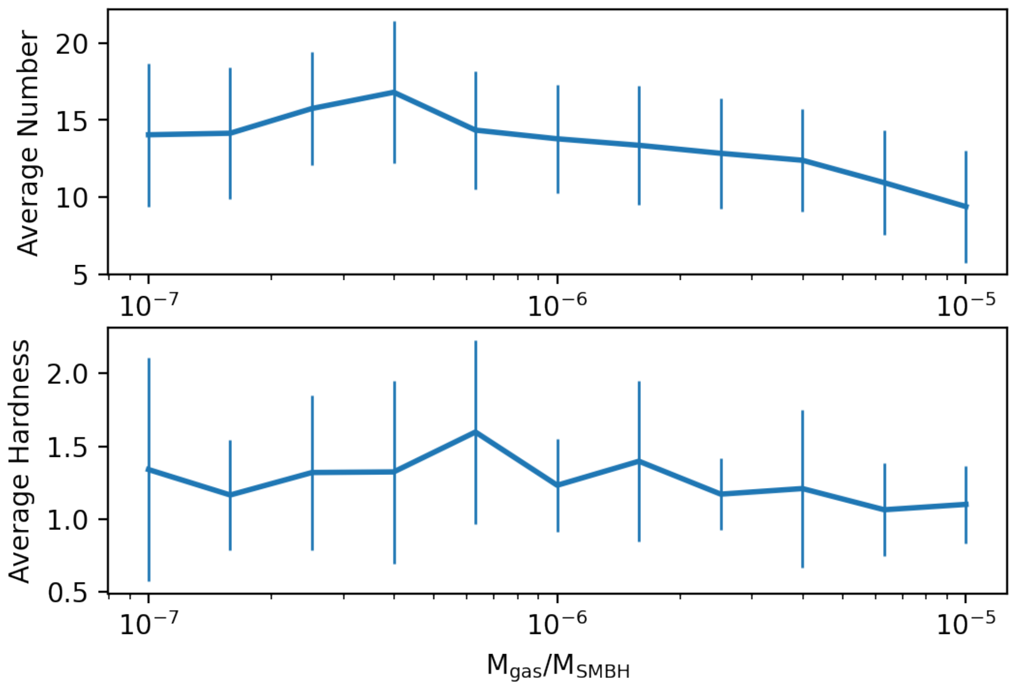

Figure 5: Top: the average number of BBHs detected in the 20 runs of each $M_{\rm gas}$. The standard deviation is shown as vertical lines. Below: the same for the average hardness of the detected BBHs.

3.2 Changing the Gas Disk

Since the results of N-body and Bridge simulations show dramatic difference, we wonder how different gas disks would affect the BBH formation efficiency.

Figure 5 shows the average and std of the number (top panel) and hardness (bottom panel) of BBHs as a function of $M_{\rm gas}$ while fixing $N_{\rm gas}$. The most remarkable result is that the std of the number of BBHs and hardness are significant. The error bars of the number of BBHs typically span half of the average value. The error bars of hardness are even greater: their span are usually the same as the average hardness. This implies that the BBH formation within 5 Myr is very sensitive to the initial conditions of the gas disk. In contrast, the variations of the average number and hardness as functions of $M_{\rm gas}$ are largely within the std. The average number of BBHs peaks at

$M_{\rm gas} = \times 10^{-6.4} M_{\rm SMBH}$. Although its contrast to the nearby values of $M_{\rm gas}$ is small compared with the std, it is larger than the average number when $M_{\rm gas} = 10^{-5} M_{\rm sun}$ by over one std. Therefore, we can still roughly conclude that, given a specific gas particle number, the BBH formation is the most efficient at $M_{\rm gas} = 10^{-6.4} M_{\rm sun}$ while gradually weakens when gravitational effects of the gas particles become minor, and gas disk would even restrain the BBH formation when the particles are too massive. On the other hand, the average hardness fluctuates within the std level, and it is hard to make a conclusion.

Figure 6 shows the results of varying $N_{\rm gas}$ while fixing $M_{\rm gas}$. Since the experiments are designed that the total gas masses are the same as in the previous experiments, the numbers are complex and not multiplies of 10. As a more intuitive alternative, we set the x-axis to the total mass $M_{\rm gasdisk}/M_{\rm SMBH}$. The reference value $N_{\rm gas} = 1000$ corresponds to $M_{\rm gasdisk}/M_{\rm SMBH} = 10^{-3}$, which matches $M_{\rm gas}/M_{\rm SMBH} = 10^{-6}$ in Figure 5. The std are also significant compared with the variations of the average number and hardness, and the average number peaks at $M_{\rm gasdisk} = 10^{-3.6} M_{\rm SMBH}$. Given the large std, we can roughly conclude that an intermediate number of the gas disk is the most efficient for BBH formation. However, the argument is still weak as the std is too large given 20 runs. Similarly to the previous experiments, the hardness does not show preference to any value of $M_{\rm disk}$.

4 Conclusions and Discussions

In our simulations, the physical properties of formed BBHs, including total mass, relative distance or velocity, angular momentum, position the disk, and hardness, are relatively stable despite the existence or change in properties of the gas disk. The gas disk can possibly enhance the formation of BBHs in galactic center when $M_{\rm disk}/M_{\rm SMBH} \sim 10^{-3.5}$ which is above 1σ significance compared to $M_{\rm disk}/M_{\rm SMBH} \sim 10^{-2}$.

The mass of the gas disk is given as $M_{\rm disk} = N_{\rm gas} M_{\rm gas}$. Since using particles to represent gas brings only gravitational effects to the BH particles, theoretically they simply provide channels to dissipate the energies of the BHs by gravitational interactions. We have found that an intermediate mass of gas particles is the most efficient for BBH formation, while the number of gas particles shows only non-significant trend, which possibly implies requirements of a wider range of $N_{\rm gas}$, though the choice of $N_{\rm gas}$ is limited by

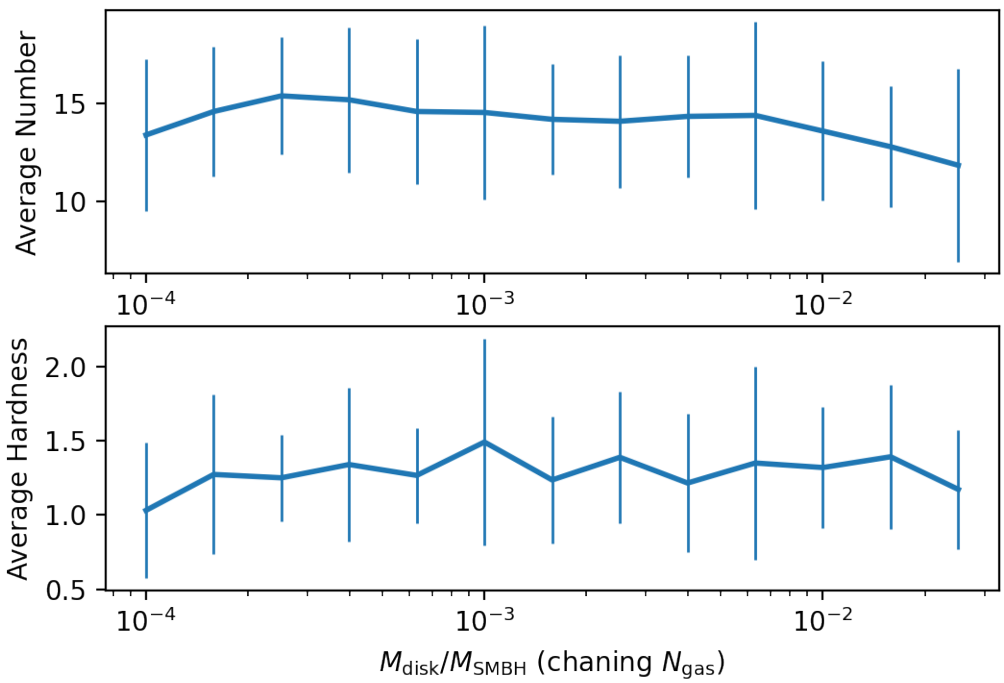

Figure 6: Top: the average number of BBHs detected in the 20 runs of changing N_{gas} while fixing M_{gas}. We use the $M_{\mathrm{gasdisk}} = N_{\mathrm{gas}} M_{\mathrm{gas}}$ as the x-axis as it is more matched to the 10-multiply values and also the total masses in Figure 5. The standard deviation is shown as vertical lines. Below: the same for the hardness of the detected BBHs.

the computation time.

Our simulations have some limitations. In reality, the interaction between the BHs and the gaseous environment includes gravitation, pressure, and accretion. The gas model in our simulation does not take the latter two into account. More time given, we may be able to perform the simulation with the effect of pressure and accretion, a higher number of gas particles, and better accuracy.

References

B. P. Abbott, R. Abbott, et al., LIGO Scientific Collaboration, and Virgo Collaboration. Observation of Gravitational Waves from a Binary Black Hole Merger. *Physics Review Letter*, 116(6):061102, February 2016. doi: 10.1103/PhysRevLett.116.061102.

B. P. Abbott, et al., LIGO Scientific Collaboration, and Virgo Collaboration. GWTC-1: A Gravitational-Wave Transient Catalog of Compact Binary Mergers Observed by LIGO and Virgo during the First and Second Observing Runs. *Physical Review X*, 9(3):031040, July 2019. doi: 10.1103/PhysRevX.9.031040.

R. Abbott, et al., LIGO Scientific Collaboration, and Virgo Collaboration. GWTC-2: Compact Binary Coalescences Observed by LIGO and Virgo during the First Half of the Third Observing Run. *Physical Review X*, 11 (2):021053, April 2021. doi: 10.1103/PhysRevX.11.021053.

The LIGO Scientific Collaboration, the Virgo Collaboration, and the KAGRA Collaboration. GWTC-3: Compact Binary Coalescences Observed by LIGO and Virgo During the Second Part of the Third Observing Run. *arXiv e-prints*, art. arXiv:2111.03606, November 2021.

Simon F. Portegies Zwart and Stephen L. W. McMillan. Black Hole Mergers in the Universe. *The Astrophysical Journal Letters*, 528(1):L17–L20, January 2000. doi: 10.1086/312422.

B. McKernan, K. E. S. Ford, and et al. Intermediate mass black holes in AGN discs - I. Production and growth. *Monthly Notices of the Royal Astronomical Society*, 425(1):460–469, September 2012. doi: 10.1111/j.1365-2966.2012.21486.x.

B. McKernan, K. E. S. Ford, and et al. Intermediate-mass black holes in AGN discs - II. Model predictions and observational constraints. *Monthly Notices of the Royal Astronomical Society*, 441(1):900–909, June 2014. doi: 10.1093/mnras/stu553.

Ilya Mandel and Selma E. de Mink. Merging binary black holes formed through chemically homogeneous evolution in short-period stellar binaries. *Monthly Notices of the Royal Astronomical Society*, 458(3):2634–2647, May 2016. doi: 10.1093/mnras/stw379.

Pablo Marchant, Norbert Langer, and et al. A new route towards merging massive black holes. *Astronomy and Astrophysics*, 588:A50, April 2016. doi: 10.1051/0004-6361/201628133.

Bin Liu, Dong Lai, and Yi-Han Wang. Black Hole and Neutron Star Binary Mergers in Triple Systems. II. Merger Eccentricity and Spin-Orbit Misalignment. *Astrophysical Journal*, 881(1):41, August 2019. doi: 10.3847/1538-4357/ab2dfb.

Simon Portegies Zwart and Steve McMillan. *Astrophysical Recipes; The art of AMUSE*. 2018. doi: 10.1088/978-0-7503-1320-9.

S. Portegies Zwart, S. L. W. McMillan, E. van Elteren, I. Pelupessy, and N. de Vries. Multi-physics simulations using a hierarchical interchangeable software interface. *Computer Physics Communications*, 184(3):456–468, March 2013. doi: 10.1016/j.cpc.2012.09.024.

F. I. Pelupessy, A. van Elteren, N. de Vries, S. L. W. McMillan, N. Drost, and S. F. Portegies Zwart. The Astrophysical Multipurpose Software Environment. *Astronomy and Astropysics*, 557:A84, September 2013. doi: 10.1051/0004-6361/201321252.

Simon Portegies Zwart, Steve McMillan, Stefan Harfst, and et al. A multiphysics and multiscale software environment for modeling astrophysical systems. *New Astronomy*, 14(4):369–378, May 2009. doi: 10.1016/j.newast.2008.10.006.

Lars Hernquist and Neal Katz. TREESPH: A Unification of SPH with the Hierarchical Tree Method. *The Astrophysical Journal Supplement*, 70:419, June 1989. doi: 10.1086/191344.

F. I. Pelupessy, P. P. van der Werf, and V. Icke. Periodic bursts of star formation in irregular galaxies. *Astronomy and Astrophysics*, 422:55–64, July 2004. doi: 10.1051/0004-6361:20047071.

F. I. Pelupessy. *Numerical studies of the interstellar medium on galactic scales*. PhD thesis, Leiden Observatory, March 2005.

J. P. E. Gerritsen and V. Icke. Star formation in N-body simulations. I. The impact of the stellar ultraviolet radiation on star formation. *Astronomy and Astrophysics*, 325:972–986, September 1997.

GRAVITY Collaboration, R. Abuter, A. Amorim, and et al. A geometric distance measurement to the Galactic center black hole with 0.3% uncertainty. *Astronomy and Astrophysics*, 625:L10, May 2019. doi: 10.1051/0004-6361/201935656.

Edwin E. Salpeter. The Luminosity Function and Stellar Evolution. *Astrophysical Journal*, 121:161, January 1955. doi: 10.1086/145971.